

SpatialFlow: Bridging All Tasks for Panoptic Segmentation

Qiang Chen^{1,2}, Anda Cheng^{1,2}, Xiangyu He^{1,2}, Peisong Wang¹, Jian Cheng^{1,2}

¹NLPR, Institute of Automation, Chinese Academy of Sciences

²University of Chinese Academy of Sciences

{qiang.chen, xiangyu.he, peisong.wang, jcheng}@nlpr.ia.ac.cn
chenganda2017@ia.ac.cn

Abstract

The newly proposed panoptic segmentation task, which aims to encompass the tasks of instance segmentation (for things) and semantic segmentation (for stuff), is an essential step toward real-world vision systems and has attracted a lot of attention in the vision community. Recently, several works have been proposed for this task. Most of them focused on unifying two tasks by sharing the backbone but ignored to highlight the significance of fully interweaving features between tasks, such as providing the spatial context of objects to both semantic and instance segmentation. However, being well aware of locations of objects is fundamental to many vision tasks, e.g., object detection, instance segmentation, semantic segmentation. In this paper, we propose object spatial information flows, which can bridge all tasks together by delivering the spatial context from the box regression task to others. Based on these flows, we present a location-aware and unified framework for panoptic segmentation, *SpatialFlow*. The spatial information flows in *SpatialFlow* can provide clues for segmenting both things and stuff and help networks better understand the whole image. Moreover, instead of endowing Mask R-CNN with a stuff segmentation branch on a shared backbone, we design four parallel sub-networks for sub-tasks, which facilitate the feature integration among different tasks. We perform a detail ablation study on MS-COCO and Cityscapes panoptic benchmarks. Extensive experiments show that *SpatialFlow* achieves state-of-the-art results and can boost the performance of things and stuff segmentation at the same time.

1 Introduction

Real-world vision systems, such as autonomous driving or augmented reality, require a rich and complete understanding of the scene. Scene understanding is a classic vision task that has been studied in pre-deep learning era (Ladický et al. 2010; Yao, Fidler, and Urtasun 2012). As the results of instance and semantic segmentation have been rapidly improved by deep learning over a short period of time and to drive deep vision algorithms a step further toward real-world, (Kirillov et al. 2018) proposed the panoptic segmentation task to unify instance and semantic segmentation, as

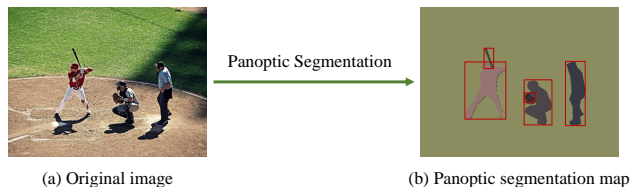


Figure 1: An illustration of the panoptic segmentation task. We also provide the box for each object.

illustrated in Figure 1. In this task, countable objects, such as people, animals, tools, are considered as *things*, and amorphous regions of similar texture or material, such as grass, sky, road, are referred to *stuff*. In (Kirillov et al. 2018), the authors used two independent models, Mask R-CNN (He et al. 2017) and PSPNet (Zhao et al. 2017), for things and stuff segmentation¹ respectively, then they used a heuristic post-processing method to merge the two outputs. Recently, several unified frameworks (de Geus, Meletis, and Dubbelman 2018; Li et al. 2018a; Kirillov et al. 2019; Li et al. 2018b; Xiong et al. 2019; Liu et al. 2019) had been proposed for panoptic segmentation. Most of them focused on unifying two tasks by sharing the backbone but ignored to highlight the significance of interweaving features between tasks, such as providing the spatial context of objects to both things and stuff segmentation.

However, being well aware of locations of objects is fundamental to many vision tasks, e.g., object detection (Ren et al. 2015; Dai et al. 2016; Lin et al. 2017b), instance segmentation (He et al. 2017; Fu, Shvets, and Berg 2019), semantic segmentation (Chen et al. 2018b; Chen et al. 2017; Zhao et al. 2017). As a combination of these tasks, panoptic segmentation can benefit from interweaving spatial features between sub-tasks. To fully leverage the reciprocal relationship among detection, things segmentation, and stuff segmentation, we carefully consider two main aspects when designing a new unified framework for panoptic segmentation

¹Refer to instance segmentation and semantic segmentation, in this paper, we use the things and the stuff to emphasize the tasks in panoptic segmentation.

task.

First, utilizing the underlying relationship in spatial dimension among tasks. As shown in Figure 1 (b), all sub-tasks in panoptic segmentation are related to locations of objects: object detection aims to localize and recognize objects; things segmentation focuses on predicting a segmentation mask for each instance relying on the box location predicted by detectors; stuff segmentation assigns class labels to the pixels which are outside of objects in the image. Based on mentioned above, we can build a global view of image segmentation by considering locations of objects.

Second, integrating features of different tasks in pixel-level. Although things and stuff segmentation are complementary tasks, their activate features are inconsistent - things segmentation is dominated by instance-level features, while stuff segmentation is influenced by pixel-level features. There is a gap in directly integrating the features of two tasks. More importantly, instances can be overlapping (Kirillov et al. 2018), which makes it hard to map instance-level features back to pixel-level. Fortunately, the features are in the format of pixel-level before they are cropped by RoIAlign (He et al. 2017) or RoIPool (Girshick 2015) layer in things segmentation. It is intuitive to implement feature integration between two tasks in pixel-level.

To this end, we present a location-aware and unified framework for panoptic segmentation, named *SpatialFlow*. We propose object spatial information flows to bridge all tasks by delivering the spatial context from box regression task to others. Moreover, instead of endowing Mask R-CNN (He et al. 2017) with a stuff segmentation branch, our *SpatialFlow* extends RetinaNet (Lin et al. 2017b). To strengthen the information flow among tasks, we design four parallel sub-networks for sub-tasks, as demonstrated in Figure 2. The overall design fully leverages spatial context and interweaves all tasks by integrating features among them, leading to better refinement of features, more robust representations for image segmentation, and better prediction results.

SpatialFlow proves its competitive performance through comparison with the state-of-the-art on MS-COCO (Lin et al. 2014) and Cityscapes (Cordts et al. 2016) benchmarks. Also, we perform a detail ablation study on various components; extensive experimental results show that the components of *SpatialFlow* can boost the performance of things and stuff segmentation at the same time.

2 Related Works

Instance Segmentation. Instance segmentation, also named as things segmentation in this paper, is a task that requires a pixel-level mask for each instance. Existing methods can be divided into two main categories, segmentation-based and region-based methods. Segmentation-based approaches, such as (Zhang, Fidler, and Urtasun 2016; Wu, Shen, and Hengel 2016), first generate a pixel-level segmentation map over the image and then perform grouping to identify object instances. While region-based methods, such as (He et al. 2017; Liu et al. 2018; Chen et al. 2019), are closely related to object detection algorithms. They predict the instance masks within the

bounding boxes generated by detectors. Region-based methods can achieve higher performance than their segmentation-based counterparts, which motivate us to resort to the region-based methods. In *SpatialFlow*, we add a mask branch on RetinaNet for instance segmentation.

Semantic Segmentation. Fully convolutional networks are essential to semantic segmentation (Long, Shelhamer, and Darrell 2015), and its variants achieve state-of-the-art results on various benchmarks. It has been proven that contextual information plays a vital role in segmentation (Motlaghi et al. 2014). A bunch of works followed this idea: Dilated convolution (Yu and Koltun 2015) was invented to keep feature resolution and maintain contextual details; Deeplab series (Chen et al. 2018b; Chen et al. 2017) proposed Atrous Spatial Pyramid Pooling (ASPP) to capture global and multi-scale contextual information; PSPNet (Zhao et al. 2017) used spatial pyramid pooling to collect contextual priors; the encoder-decoder networks (Ronneberger, Fischer, and Brox 2015; Noh, Hong, and Han 2015) are designed to capture contextual information in encoder and gradually recover the details in decoder. Our *SpatialFlow*, built upon FPN (Lin et al. 2017a), uses an encoder-decoder architecture for stuff segmentation to capture the contextual information. We take the spatial context of object detection into consideration and build a connection for things and stuff segmentation.

Panoptic Segmentation. The panoptic segmentation task was proposed in (Kirillov et al. 2018), where the authors provided a baseline method with two separate networks, then used a heuristic post-processing method to merge two outputs. Later, Li et al. (Li, Arnab, and Torr 2018) followed this task and proposed a weakly- and semi-supervised panoptic segmentation method. Recently, a number of unified frameworks had been proposed: De Geus et al. (de Geus, Meletis, and Dubbelman 2018) used a shared backbone for both things and stuff segmentation; Li et al. (Li et al. 2018a) proposed a unified network named TASCNet by considering things and stuff consistency; Li et al. (Li et al. 2018b) proposed AUNet which utilized the attention module to capture the complementary information delivered by things and stuff; Kirillov et al. (Kirillov et al. 2019) introduced PanopticFPN by endowing Mask R-CNN (He et al. 2017) with a stuff branch; Liu et al. (Liu et al. 2019) designed a spatial ranking module to deal with the occlusion problem between the predicted instances; Xiong et al. (Xiong et al. 2019) proposed a parameter-free panoptic head to resolve the conflicts between things and stuff segmentation; Yang et al. (Yang et al. 2019) present a single-shot, bottom-up approach for panoptic segmentation. However, most of these methods ignored to highlight the significance of interweaving features between tasks. Our *SpatialFlow* helps build a panoptic view for image segmentation by information flows.

3 SpatialFlow

We present a location-aware and unified framework for panoptic segmentation. The sketch of our network is illus-

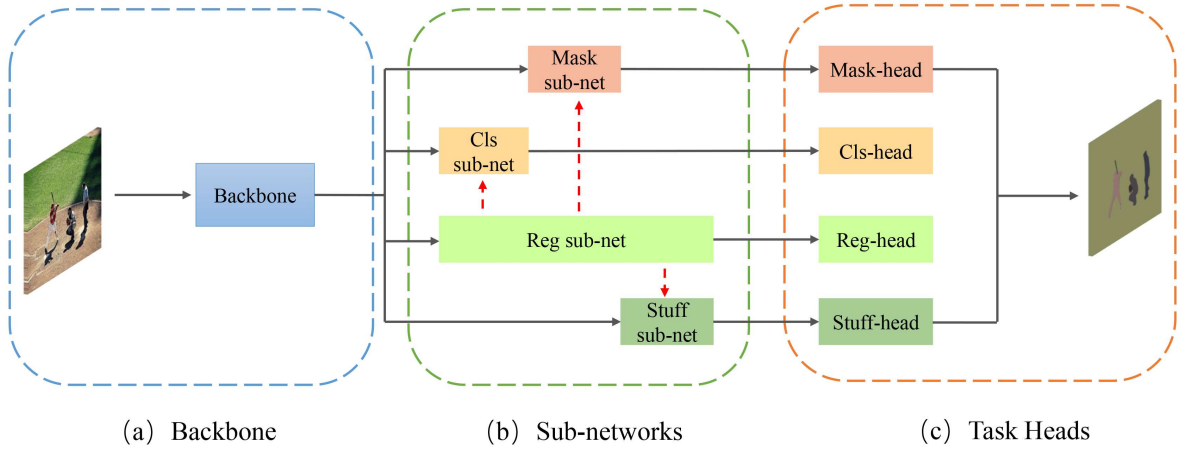


Figure 2: An illustration of the overall architecture. The SptailFlow consists of three parts: (a) Backbone with FPN. (b) Four parallel sub-networks: We propose the spatial information flow and feature fusion between tasks in this part. The spatial flows are illustrated as red dashed arrows, and the feature fusion is not shown in this figure for an elegant presentation; (c) Four heads for specific tasks: The Cls-head and Reg-head predict detection box together for Mask-head. The final result of SpatialFlow is a combination of the outputs of Mask-head and Stuff-head.

trated in Figure 2. The SpatialFlow can be divided into three parts: a backbone with FPN, four parallel sub-networks, and four task-specific heads. In this section, we describe the details of the major components in each part.

3.1 Backbone

The backbone contains FPN, whose outputs are five levels of features named $\{P_3, P_4, P_5, P_6, P_7\}$ with a downsample rate of 8, 16, 32, 64, 128 respectively. In FPN, all features have 256 channels. The details are shown in the blue dashed rectangle of Figure 3, P_6 is obtained via a 3×3 stride-2 convolution on C_5 , and P_7 is computed by applying ReLU followed by a 3×3 stride-2 conv on P_6 . Following (Fu, Shvets, and Berg 2019), we treat these features differently against various tasks: we use all the five levels to predict the bounding boxes in detection but only send $\{P_3, P_4, P_5\}$ to mask and stuff sub-networks.

3.2 Parallel sub-networks

RetinaNet-based framework. To deal with the panoptic segmentation task, we begin with RetinaNet. We first add a mask head for things segmentation and tackle stuff segmentation with a stuff head. Under this assumption, there are only two sub-networks - classification sub-network (cls sub-net for short) and regression sub-network (reg sub-net for short) - in this part. The operations in the sub-networks, which transform the features of FPN to the inputs of downstream heads, can be formulated as follows:

$$\begin{aligned} P_{reg_{i,j}} &= \zeta(P_{reg_{i,j-1}}), & P_{cls_{i,j}} &= \zeta(P_{cls_{i,j-1}}); \\ P_{reg_{i,0}} &= P_i, & P_{cls_{i,0}} &= P_i; \\ P_{mask_i} &= P_i, & P_{stuff_i} &= P_i. \end{aligned} \quad (1)$$

Here, i represents the level index of feature, P_i is the i -th level output of FPN, and $i \in \{3, 4, 5, 6, 7\}$ in reg sub-

net and cls sub-net while $i \in \{3, 4, 5\}$ for mask and stuff; j indicates the index of feature map in sub-networks, and $j \in \{1, 2, 3, 4\}$ in reg sub-net and cls sub-net; $\zeta(\cdot)$ denotes a block that contains a convolution and a ReLU layer.

Stuff and Mask sub-networks. In the architecture discussed above, there is no direct path for the spatial information to flow across tasks, which prevents further improvements on both things and stuff segmentation. In SpatialFlow, we consider the spatial information for all tasks. To improve the information flow, we design a stuff sub-network, which is parallel to reg sub-net and consists of four Conv-ReLU blocks. Moreover, to avoid the inconsistency between instance-level and pixel-level features, we propose to add a mask sub-network with one Conv-ReLU block. The integrations between features are in pixel-level. Until now, between the FPN and the task-specific heads, there are four parallel sub-networks. We present the modifications in architecture below:

$$\begin{aligned} P_{reg_{i,j}} &= \zeta(P_{reg_{i,j-1}}), & P_{cls_{i,j}} &= \zeta(P_{cls_{i,j-1}}); \\ P_{mask_{i,1}} &= \zeta(P_i), & P_{stuff_{i,j}} &= \zeta(P_{stuff_{i,j-1}}); \\ P_{reg_{i,0}} &= P_i, & P_{cls_{i,0}} &= P_i, & P_{stuff_{i,0}} &= P_i. \end{aligned} \quad (2)$$

where $j \in \{1, 2, 3, 4\}$ in stuff sub-net. We directly use $P_{mask_{i,1}}$ to represent the output feature of mask sub-net as there is only one Conv-ReLU block.

Spatial information flow. We carefully consider two main aspects to make all tasks location-aware: (1) Being well aware of object locations is fundamental to many vision tasks (He et al. 2017), such as object detection, instance segmentation, semantic segmentation. (2) All sub-tasks in panoptic segmentation are related to the locations of objects.

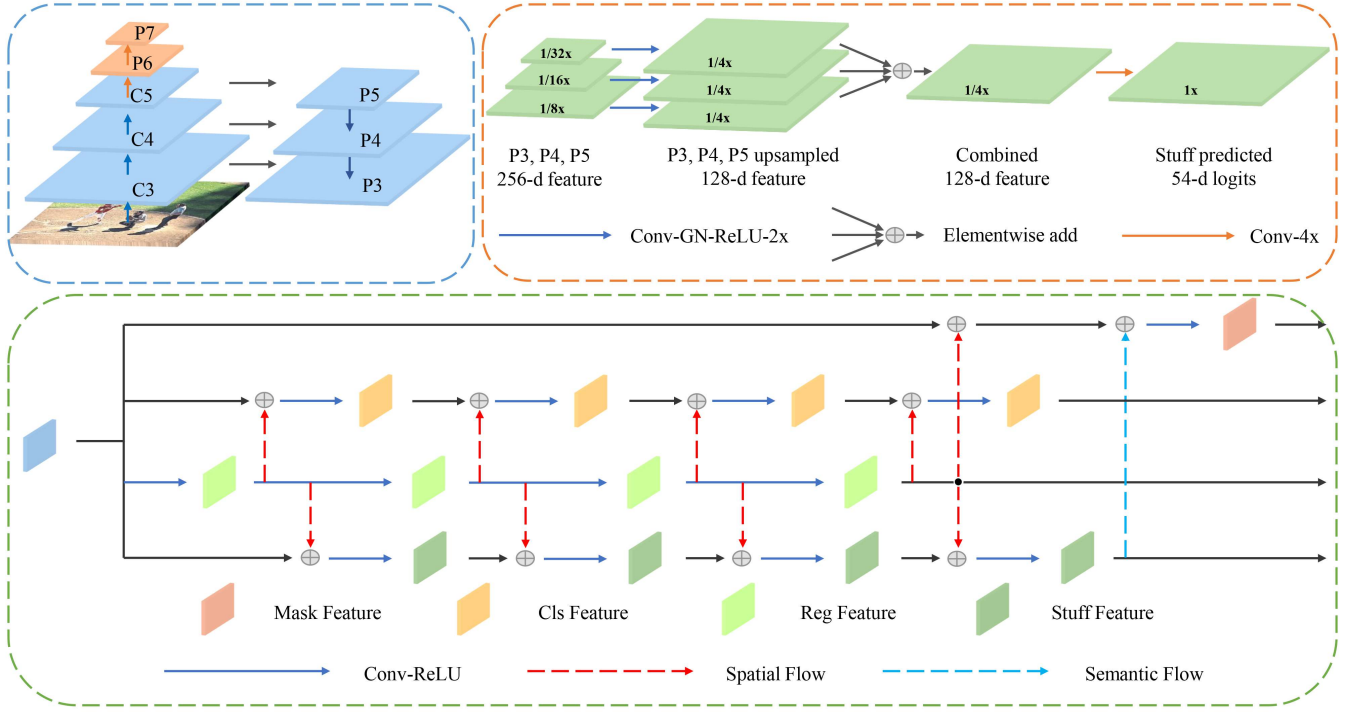


Figure 3: The designs for each part in SpatialFlow. In the blue dashed rectangle, we show the outputs of FPN, which are the features named $\{P_3, P_4, P_5, P_6, P_7\}$. In the orange dashed rectangle, we present the architecture of the stuff head. More importantly, all the information flows in sub-networks are illustrated in the green dashed box.

With the help of the spatial context, the features can be more discriminative, which further boosts the performance. Furthermore, things and stuff segmentation are complementary tasks, which indicates that the semantic feature in the stuff sub-net will be a benefit to the mask segmentation by providing additional context.

Thus, we propose a four parallel sub-networks design, then add the spatial information flow to all tasks and deliver the stuff semantic feature to mask sub-net, as shown in the green dashed box of Figure 3. We obtain a final version of our sub-networks, which can be implemented as follows:

$$\begin{aligned}
 P_{reg_{i,j}} &= \zeta(P_{reg_{i,j-1}}), & P_{cls_{i,j}} &= \zeta(P_{cls_{i,j-1}} + \phi(P_{reg_{i,j}})); \\
 P_{stuff_{i,j}} &= \zeta(P_{stuff_{i,j-1}} + \phi(P_{reg_{i,j}})); \\
 P_{mask_{i,1}} &= \zeta(P_i + \phi(P_{reg_{i,4}}) + \psi(P_{stuff_{i,4}})); \\
 P_{reg_{i,0}} &= P_i, & P_{cls_{i,0}} &= P_i, & P_{stuff_{i,0}} &= P_i.
 \end{aligned} \tag{3}$$

Here, $\phi()$ denotes an adaptation convolution from box regression task to others; $\psi()$ denotes a adaption convolution from stuff sub-net to mask sub-net. We use a 3×3 convolution layer for both $\phi()$ and $\psi()$. To generate $P_{mask_{i,1}}$, we deliver $P_{reg_{i,4}}$ and $P_{stuff_{i,4}}$, which are the last features of reg and stuff sub-net, to the feature P_i in the mask sub-net. All features have 256 channels in this part.

3.3 Task-specific heads

As illustrated in the orange dashed box of Figure 2, we use four heads for box classification, box regression, things segmentation, and stuff segmentation respectively. To generate the final output of SpatialFlow, we first obtain the detection results by considering the outputs of reg head and cls head jointly, then make segmentation mask predictions for all instances based on the predicted boxes; at the same time, we generate stuff segmentation map by applying stuff head; finally, we implement a heuristic post-processing method (Kirillov et al. 2019) to merge the things and stuff segmentation results.

In cls and reg head, we apply a 3×3 convolution to the outputs of cls and reg sub-nets. In mask head, we adopt the same design as Mask R-CNN (He et al. 2017), which consists of a RoIAlign layer, four consecutive 3×3 convolutions, a 3×3 transposed convolution and a 1×1 prediction convolution. The stuff head is shown in the orange dashed box of Figure 3. After stuff sub-net, we obtain three feature maps with scales of $1/8$, $1/16$, $1/32$ of the original image. We perform upsampling on each feature map gradually by blocks, each of which contains a 3×3 convolution, a group norm (Wu and He 2018) layer, a ReLU layer and a $2 \times$ bilinear upsampling operation. All the features are upsampled to the scale of $1/4$, which are then element-wise summed. A final 1×1 convolution, a $4 \times$ bilinear upsampling operation and a softmax are applied to get the segmentation result.

3.4 Implementation Details

Training. As a unified framework for panoptic segmentation, there are four different losses for SpatialFlow to optimize during the training stage. The loss function can be formulated as follow:

$$\mathcal{L} = (\mathcal{L}_{cls} + \mathcal{L}_{reg} + \mathcal{L}_{mask}) + \lambda \cdot \mathcal{L}_{stuff} \quad (4)$$

where \mathcal{L}_{cls} , \mathcal{L}_{reg} and \mathcal{L}_{mask} belong to the things segmentation task, and \mathcal{L}_{stuff} is the loss of the stuff segmentation. We add a hyper-parameter λ to balance the losses between things and stuff segmentation. We implement our SpatialFlow with a toolbox (Chen et al. 2018a) based on PyTorch (Paszke et al. 2017).

We inherit all the hyper-parameters from RetinaNet except that we set the threshold of NMS to 0.4 when generating proposals during training. For mask prediction, we add the ground truth boxes to the proposals set and run the mask head for all proposals. For training strategies, we fix the batch norm layer in the backbone and train our model over 4 GPUs with a total of 8 images per minibatch. On MS-COCO (Lin et al. 2014), all models are trained for 20 epochs with an initial learning rate of 5×10^{-3} , which is decreased by 10 after 16 and 19 epochs; on Cityscapes (Cordts et al. 2016), we set the initial learning rate as 1.25×10^{-2} and the number of epochs as 176, then drop the learning rate by 10 on the 112th and the 152th epoch. For image size, we resize the shorter edge of the image to 600 pixels and 800 pixels on COCO, while on Cityscapes, we adopt 512×1024 image crops after scaling each image by 0.5 to $2.0 \times$. As Kirillov et al. (Kirillov et al. 2019) did, we also predict a particular ‘other’ class for all things categories in stuff head on COCO benchmark.

Inference. Our model follows a pipeline in the inference stage: (1) generate the detection results; (2) obtain the maps of things and stuff segmentation; (3) merge the two outputs to form a final panoptic segmentation map. In detection, we set the threshold of NMS to 0.4 for each class separately, and choose the top-100 scoring bounding boxes to send to mask head. During merging, we first ignore the stuff regions labeled ‘other’; then we resolve the overlap problem between instances based on their scores; at last, we merge the things and stuff map in favor of things.

4 Experiments

4.1 Dataset and Evaluation metric

Dataset. We evaluate our model on both COCO (Lin et al. 2014) and Cityscapes (Cordts et al. 2016). COCO consists of 80 things and 53 stuff classes. We use the 2017 data splits with 118k/5k/20k *train/val/test* images. We use *train* split for training, and report leison and sensitive studies by evaluating on *val* split. For our main results, we report our panoptic performance on the *test-dev* split. Cityscapes has 5k high-resolution images with fine pixel-accurate annotations: 2975 train, 500 val, and 1525 test. There are 19 classes on Cityscapes, 8 with instance-level masks. For all experiments, we report our performance on *val* split with 11 stuff classes and 8 things classes.

Evaluation metric. We adopt the *panoptic quality* (PQ) as the metric. As proposed in (Kirillov et al. 2018), PQ can be formulated as follow:

$$PQ = \underbrace{\frac{\sum_{(p,g) \in TP} IoU(p,g)}{|TP|}}_{\text{segmentation quality (SQ)}} \times \underbrace{\frac{|TP|}{|TP| + \frac{1}{2}|FP| + \frac{1}{2}|FN|}}_{\text{recognition quality (RQ)}} \quad (5)$$

where p and g are predicted and ground truth segments, TP (true positives), FP (false positives), and FN (false negatives) represent matched pairs of segments ($IoU(p,g) > 0.5$), unmatched predicted segments, and unmatched ground truth segments, respectively. Besides, PQ can be explained as the multiplication of a segmentation quality (SQ) and a recognition quality (RQ). We also use SQ and RQ to measure the performance in our experiments.

4.2 Ablation studies

In this section, we carefully design various experiments to reveal the contribution of each component in our unified framework. We adopt the Retina-based framework as our baseline model. All the results and discussions are presented below.

λ	PQ	PQ Th	PQ St
1.0	37.5	41.8	30.9
0.75	38.2	43.0	31.1
0.5	38.8	44.0	31.0
0.4	38.9	44.3	30.8
0.3	39.1	44.5	30.9
0.25	39.3	45.1	30.5
0.2	39.0	44.9	30.0
0.1	38.5	45.1	28.5

Table 1: The results of the baseline model on COCO *val* split with different values of λ based on ResNet-50 with an image size of 600px.

model	PQ	PQ Th	PQ St
baseline	39.7	46.0	30.2
+ stuff + mask sub-net	40.3	46.2	31.4
+ reg-cls flow	40.5	46.6	31.4
+ reg-stuff flow	40.7	46.3	32.0
+ reg-mask flow	40.7	46.4	31.8
+ stuff-mask flow	40.9	46.8	31.9

Table 2: The contribution of each component in SpatialFlow with ResNet-50 and an image size of 800px on COCO *val* split. Each row adds an extra component to the above row.

Multi-Task training. We perform multi-task training on panoptic segmentation by tackling things and stuff simultaneously. However, there is an inconsistency between the gradients of things and stuff segmentation (Liu et al. 2019), which is caused by the different objectives of two tasks - things segmentation tries to optimize the instance-level

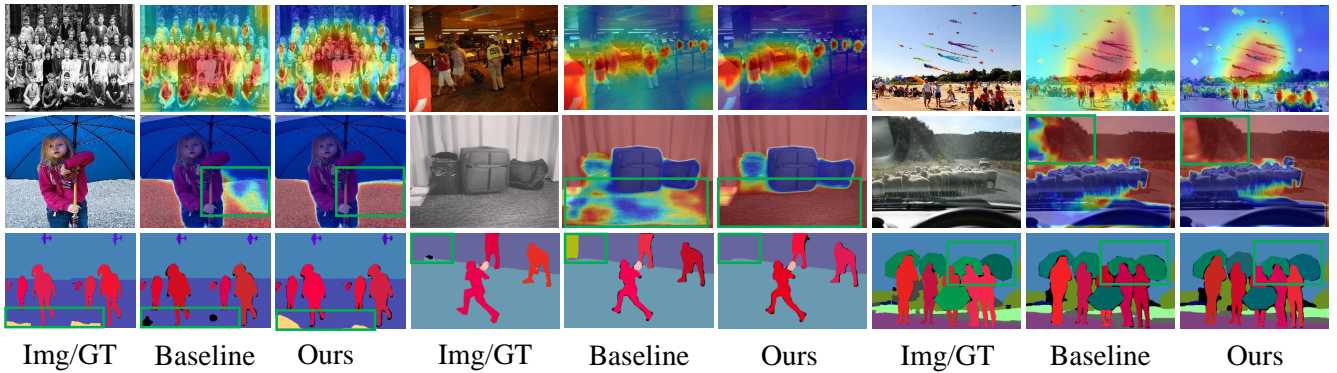


Figure 4: We present cls-head and stuff-head heatmap in first two rows, then illustrate the panoptic map in the third row.

model	PQ	PQ^{Th}	PQ^{St}
baseline	57.3	53.5	60.0
+ stuff + mask sub-net	57.5	53.6	60.3
+ reg-cls flow	58.0	55.1	60.1
+ reg-stuff flow	58.3	54.6	60.9
+ reg-mask flow	58.5	54.7	61.3
+ stuff-mask flow	58.6	54.9	61.4

Table 3: The contribution of each component in SpatialFlow with ResNet-50 on Cityscapes *val* split. Each row adds an extra component to the above row.

masks while stuff segmentation aims to learn to predict the pixel-level segmentation maps. To balance the gradients between two tasks, we search the best value for the hyperparameter λ on COCO dataset with image shorter edge of 600px. We show the results of the baseline model with various values of λ in Table 1, which are 1.0, 0.75, 0.5, 0.4, 0.3, 0.25, 0.2, 0.1. According to the results, we found that directly adding the losses together ($\lambda = 1.0$) leads to low performance, which is 37.5 PQ. We demonstrate the power of λ and discover that the best value to balance the losses is 0.25, with which the baseline model achieves 39.3 PQ and earns a 1.8 PQ gain compared with $\lambda = 1.0$. For Cityscapes dataset, we follow (Kirillov et al. 2019) and set $\lambda = 1.0$.

Stuff and Mask sub-networks. In this section, we decompose the sub-nets to make clear their effects. Table 2 shows that the sub-nets bring considerable gain on stuff segmentation, which is 1.2 PQ^{St} . In Table 3, we also discover that the sub-nets slightly bring consistency improvements on Cityscape dataset. Stuff and Mask sub-nets are designed to enlarge the region for integrating features and improve the information flow between tasks. These improvements demonstrate their additional function that can help the model learn better representations.

Spatial information flow. We conduct experiments to highlight the significance of fully interweaving features between tasks in this section. We propose the spatial information flows to connect all the tasks. There are three paths to deliver the spatial context from box regression task to oth-

Backbone	size	PQ	PQ^{Th}	PQ^{St}
ResNet-50	600px	40.3	45.6	32.2
ResNet-101	600px	41.2	46.6	32.9
ResNet-50	800px	40.9	46.8	31.9
ResNet-101	800px	42.2	48.2	33.1

Table 4: The results of SpatialFlow on COCO *val* split with different backbones and various image sizes.

ers: the path from the reg sub-net to the cls sub-net (reg-cls flow), the path to the stuff sub-net (reg-stuff flow), and the path to the mask sub-net (reg-mask flow). The results are reported in Table 2 and Table 3. At first, we add the reg-cls path, and we obtain a 0.4 PQ^{Th} improvement on COCO and a 1.5 PQ^{Th} gain on Cityscapes, which is brought by better detection results. Adding spatial context helps cls sub-net to extract discriminative features, which is essential for detection. Then we build a spatial path for stuff sub-net, as shown in the 5th row of Table 2 and Table 3, we earn a 0.6 PQ^{St} gain on COCO and a 0.8 PQ^{St} gain compared with the former model, which indicates that the spatial context helps segment stuff more accurately. The reg-mask path and the semantic path also show their effectiveness on both things and stuff segmentation. Comparing with the original model, SpatialFlow can achieve a consistent gain in both things and stuff. The results prove the significance of the spatial context in panoptic segmentation to some extent. It is worth noting that we only apply the element-wise sum operation to integrate the spatial context in this work. We believe that we can get a greater improvement by implementing attention modules. We also show the results of different image sizes and different backbones on COCO in Table 4. We find that the stuff segmentation is robust to the image size, while things segmentation benefits from large image sizes. Our SpatialFlow can achieve 42.2 PQ with a single ResNet-101 backbone on the *val* split. Also, SpatialFlow can process 10 images per second during inference with an image size of 600×1000 on a single Tesla V100 GPU.

From quantitative improvements to qualitative difference. In this section, we want to find out how the quantitative improvements translate to the qualitative difference in SpatialFlow. In Figure 4, we choose to study the models

model	backbone	image size	PQ	PQ Th	PQ St	SQ	RQ
JSIS-Net (2018)	ResNet-50	400 × 400	27.2	29.6	23.4	71.9	35.9
DeeperLab (2019)	Xception-71	321 × 321	34.3	37.5	29.6	77.1	43.1
PanopticFPN (2019)	ResNet-101-FPN	[640, 800]	40.9	48.3	29.7	-	-
OANet (2019)	ResNet-101-FPN	800 × 1333	41.3	50.4	27.7	-	-
SpatialFlow	ResNet-101-FPN	600 × 1000	41.8	47.6	33.0	79.2	51.0
SpatialFlow	ResNet-101-FPN	800 × 1333	42.8	49.1	33.1	78.9	52.1

Table 5: Comparison to the state-of-the-art methods on COCO 2018 *test-dev* split. In the table, ‘[640, 800]’ represents multi-scale training with shorter image side in [640, 800]. We only compare to the methods without deformable convolutions here.

model	backbone	PQ	PQ Th	PQ St	SQ	RQ
Megvii (Face++)	ensemble model	53.2	62.2	39.5	83.2	62.9
Caribbean	ensemble model	46.8	54.3	35.5	80.5	57.1
PKU 360	ResNeXt-152-DCN	46.3	58.6	27.6	79.6	56.1
AUNet (2018b)	ResNeXt-152-DCN	46.5	55.9	32.5	81.0	56.1
UPSNet (2019)	ResNet-101-DCN	46.6	53.2	36.7	80.5	56.9
SpatialFlow	ResNet-101-DCN	47.3	53.5	37.9	81.8	56.9

Table 6: Comparison to the state-of-the-art methods on COCO 2018 *test-dev* split. In this table, we report our results with deformable convolution and multi-scale testing. For the implementation details, please refer to the Supplementary File. The top 3 rows contain results of top 3 models taken from the official leaderboard.

model	PQ	PQ Th	PQ St
PanopticFPN-101 (2019)	58.1	52.0	62.5
AUNet-101 (2018b)	59.0	54.8	62.1
TASCNet-101-COCO (2018a)	59.2	56.0	61.5
UPSNet-101-COCO-M (2019)	61.8	57.6	64.8
SpatialFlow-101	59.6	55.0	63.1
SpatialFlow-101-COCO-M	62.5	56.6	66.8

Table 7: Comparison to the state-of-the-art methods on Cityscapes *val* split. In this table, ‘-101’ represents that the backbone is ResNet-101; ‘-COCO’ means using COCO pretrain model; ‘-M’ is the multi-scale testing. The implementation details can be found in Supplementary File.

in Table 2 and visualize the last feature map in cls-head and stuff-head of both baseline and SpatialFlow via CAM (Zhou et al. 2016). The visualized heatmaps illustrate that spatial information can help things branch to focus on objects and make the stuff branch aware of the precise boundary of things and stuff. In the third row of Figure 4, by comparing the segmentation maps of SpatialFlow with those of the baseline, it is intuitive how the quantitative gains translate to visual qualitative improvements. As we can see, the spatial information flow helps the model retrieve missing stuff parts, correct the wrong prediction area, and split crowded instances.

4.3 Comparisons to the state-of-the-art

In this section, we compare our SpatialFlow to the existing methods. The results are shown in Table 5, Table 6, and Table 7. On COCO, to make a fair comparison, we report the results of different image sizes. With a single ResNet-101-FPN backbone, our SpatialFlow can achieve **41.8** PQ

and **42.8** PQ with the shorter image side of 600 pixels and 800 pixels respectively. As illustrate in Table 5, SpatialFlow outperforms PanopticFPN (Kirillov et al. 2019) by 1.9 PQ and OANet (Liu et al. 2019) by 1.5 PQ. More importantly, SpatialFlow achieves a new state-of-the-art performance on PQSt, **33.1** PQ, which outperform other models by a large margin (3.4 PQ and 5.4 PQ respectively). The results demonstrate the effectiveness of integrating features in pixel-level, which has a great impact on stuff segmentation. We also report the results with a stronger backbone in Table 6. We achieve **47.3** PQ, which is the state-of-the-art results on COCO panoptic benchmark. Moreover, we show our results on Cityscapes dataset in Table 7. Without COCO pretrain model, SpatialFlow can achieve **59.6** PQ on Cityscapes *val* split, which is 1.5 PQ and 0.6 PQ higher than PanopticFPN (Kirillov et al. 2019) and AUNet (Li et al. 2018b) respectively. With COCO pretrain model, Our SpatialFlow can achieve **62.5** PQ on Cityscapes with multi-scale testing, which is 0.7 PQ higher than UPSNet (Xiong et al. 2019). SpatialFlow achieves the state-of-the-art results on both COCO and Cityscapes benchmarks.

5 Conclusion

In this work, we propose a new location-aware and unified framework, SpatialFlow, for panoptic segmentation. We emphasize the importance of the spatial context and bridge all the tasks by building spatial information flow, then achieve state-of-the-art performance on both COCO panoptic benchmark *test-dev* split and Cityscapes panoptic benchmark *val* split, which prove the effectiveness of our model. Moreover, we only use the element-wise sum when doing feature fusion in this work, and we believe that we can achieve higher performance by introducing attention modules to SpatialFlow. In the future, we will do more investigation work on how to fully integrating features.

References

- [Chen et al. 2017] Chen, L.-C.; Papandreou, G.; Schroff, F.; and Adam, H. 2017. Rethinking atrous convolution for semantic image segmentation. *arXiv preprint arXiv:1706.05587*.
- [Chen et al. 2018a] Chen, K.; Pang, J.; Wang, J.; Xiong, Y.; Li, X.; Sun, S.; Feng, W.; Liu, Z.; Shi, J.; Ouyang, W.; Loy, C. C.; and Lin, D. 2018a. mmdetection. <https://github.com/open-mmlab/mmdetection>.
- [Chen et al. 2018b] Chen, L.-C.; Papandreou, G.; Kokkinos, I.; Murphy, K.; and Yuille, A. L. 2018b. Deeplab: Semantic image segmentation with deep convolutional nets, atrous convolution, and fully connected crfs. *IEEE transactions on pattern analysis and machine intelligence* 40(4):834–848.
- [Chen et al. 2019] Chen, K.; Pang, J.; Wang, J.; Xiong, Y.; Li, X.; Sun, S.; Feng, W.; Liu, Z.; Shi, J.; Ouyang, W.; et al. 2019. Hybrid task cascade for instance segmentation. *arXiv preprint arXiv:1901.07518*.
- [Cordts et al. 2016] Cordts, M.; Omran, M.; Ramos, S.; Rehfeld, T.; Enzweiler, M.; Benenson, R.; Franke, U.; Roth, S.; and Schiele, B. 2016. The cityscapes dataset for semantic urban scene understanding. In *Proceedings of the IEEE conference on computer vision and pattern recognition*, 3213–3223.
- [Dai et al. 2016] Dai, J.; Li, Y.; He, K.; and Sun, J. 2016. R-fcn: Object detection via region-based fully convolutional networks. In *Advances in neural information processing systems*, 379–387.
- [de Geus, Meletis, and Dubbelman 2018] de Geus, D.; Meletis, P.; and Dubbelman, G. 2018. Panoptic segmentation with a joint semantic and instance segmentation network. *arXiv preprint arXiv:1809.02110*.
- [Fu, Shvets, and Berg 2019] Fu, C.-Y.; Shvets, M.; and Berg, A. C. 2019. Retinamask: Learning to predict masks improves state-of-the-art single-shot detection for free. *arXiv preprint arXiv:1901.03353*.
- [Girshick 2015] Girshick, R. 2015. Fast r-cnn. In *Proceedings of the IEEE international conference on computer vision*, 1440–1448.
- [He et al. 2017] He, K.; Gkioxari, G.; Dollár, P.; and Girshick, R. 2017. Mask r-cnn. In *Proceedings of the IEEE international conference on computer vision*, 2961–2969.
- [Kirillov et al. 2018] Kirillov, A.; He, K.; Girshick, R.; Rother, C.; and Dollár, P. 2018. Panoptic segmentation. *arXiv preprint arXiv:1801.00868*.
- [Kirillov et al. 2019] Kirillov, A.; Girshick, R.; He, K.; and Dollár, P. 2019. Panoptic feature pyramid networks. *arXiv preprint arXiv:1901.02446*.
- [Ladický et al. 2010] Ladický, L.; Sturges, P.; Alahari, K.; Russell, C.; and Torr, P. H. 2010. What, where and how many? combining object detectors and crfs. In *European conference on computer vision*, 424–437. Springer.
- [Li, Arnab, and Torr 2018] Li, Q.; Arnab, A.; and Torr, P. H. 2018. Weakly-and semi-supervised panoptic segmentation. In *Proceedings of the European Conference on Computer Vision (ECCV)*, 102–118.
- [Li et al. 2018a] Li, J.; Raventos, A.; Bhargava, A.; Tagawa, T.; and Gaidon, A. 2018a. Learning to fuse things and stuff. *arXiv preprint arXiv:1812.01192*.
- [Li et al. 2018b] Li, Y.; Chen, X.; Zhu, Z.; Xie, L.; Huang, G.; Du, D.; and Wang, X. 2018b. Attention-guided unified network for panoptic segmentation. *arXiv preprint arXiv:1812.03904*.
- [Lin et al. 2014] Lin, T.-Y.; Maire, M.; Belongie, S.; Hays, J.; Perona, P.; Ramanan, D.; Dollár, P.; and Zitnick, C. L. 2014. Microsoft coco: Common objects in context. In *European conference on computer vision*, 740–755. Springer.
- [Lin et al. 2017a] Lin, T.-Y.; Dollár, P.; Girshick, R.; He, K.; Hariharan, B.; and Belongie, S. 2017a. Feature pyramid networks for object detection. In *Proceedings of the IEEE Conference on Computer Vision and Pattern Recognition*, 2117–2125.
- [Lin et al. 2017b] Lin, T.-Y.; Goyal, P.; Girshick, R.; He, K.; and Dollár, P. 2017b. Focal loss for dense object detection. In *Proceedings of the IEEE international conference on computer vision*, 2980–2988.
- [Liu et al. 2018] Liu, S.; Qi, L.; Qin, H.; Shi, J.; and Jia, J. 2018. Path aggregation network for instance segmentation. In *Proceedings of the IEEE Conference on Computer Vision and Pattern Recognition*, 8759–8768.
- [Liu et al. 2019] Liu, H.; Peng, C.; Yu, C.; Wang, J.; Liu, X.; Yu, G.; and Jiang, W. 2019. An end-to-end network for panoptic segmentation. *arXiv preprint arXiv:1903.05027*.
- [Long, Shelhamer, and Darrell 2015] Long, J.; Shelhamer, E.; and Darrell, T. 2015. Fully convolutional networks for semantic segmentation. In *Proceedings of the IEEE conference on computer vision and pattern recognition*, 3431–3440.
- [Mottaghi et al. 2014] Mottaghi, R.; Chen, X.; Liu, X.; Cho, N.-G.; Lee, S.-W.; Fidler, S.; Urtasun, R.; and Yuille, A. 2014. The role of context for object detection and semantic segmentation in the wild. In *Proceedings of the IEEE Conference on Computer Vision and Pattern Recognition*, 891–898.
- [Noh, Hong, and Han 2015] Noh, H.; Hong, S.; and Han, B. 2015. Learning deconvolution network for semantic segmentation. In *Proceedings of the IEEE international conference on computer vision*, 1520–1528.
- [Paszke et al. 2017] Paszke, A.; Gross, S.; Chintala, S.; Chanan, G.; Yang, E.; DeVito, Z.; Lin, Z.; Desmaison, A.; Antiga, L.; and Lerer, A. 2017. Automatic differentiation in pytorch.
- [Ren et al. 2015] Ren, S.; He, K.; Girshick, R.; and Sun, J. 2015. Faster r-cnn: Towards real-time object detection with region proposal networks. In *Advances in neural information processing systems*, 91–99.
- [Ronneberger, Fischer, and Brox 2015] Ronneberger, O.; Fischer, P.; and Brox, T. 2015. U-net: Convolutional networks for biomedical image segmentation. In *International Conference on Medical image computing and computer-assisted intervention*, 234–241. Springer.
- [Wu and He 2018] Wu, Y., and He, K. 2018. Group normalization. In *Proceedings of the European Conference on Computer Vision (ECCV)*, 3–19.
- [Wu, Shen, and Hengel 2016] Wu, Z.; Shen, C.; and Hengel, A. v. d. 2016. Bridging category-level and instance-level semantic image segmentation. *arXiv preprint arXiv:1605.06885*.
- [Xiong et al. 2019] Xiong, Y.; Liao, R.; Zhao, H.; Hu, R.; Bai, M.; Yumer, E.; and Urtasun, R. 2019. Upsnet: A unified panoptic segmentation network. *arXiv preprint arXiv:1901.03784*.
- [Yang et al. 2019] Yang, T.-J.; Collins, M. D.; Zhu, Y.; Hwang, J.-J.; Liu, T.; Zhang, X.; Sze, V.; Papandreou, G.; and Chen, L.-C. 2019. Deeplab: Single-shot image parser. *arXiv preprint arXiv:1902.05093*.
- [Yao, Fidler, and Urtasun 2012] Yao, J.; Fidler, S.; and Urtasun, R. 2012. Describing the scene as a whole: joint object detection. In *Proceedings of CVPR*. Citeseer.
- [Yu and Koltun 2015] Yu, F., and Koltun, V. 2015. Multi-scale context aggregation by dilated convolutions. *arXiv preprint arXiv:1511.07122*.

[Zhang, Fidler, and Urtasun 2016] Zhang, Z.; Fidler, S.; and Urtasun, R. 2016. Instance-level segmentation for autonomous driving with deep densely connected mrfs. In *Proceedings of the IEEE Conference on Computer Vision and Pattern Recognition*, 669–677.

[Zhao et al. 2017] Zhao, H.; Shi, J.; Qi, X.; Wang, X.; and Jia, J. 2017. Pyramid scene parsing network. In *Proceedings of the IEEE conference on computer vision and pattern recognition*, 2881–2890.

[Zhou et al. 2016] Zhou, B.; Khosla, A.; Lapedriza, A.; Oliva, A.; and Torralba, A. 2016. Learning deep features for discriminative localization. In *Proceedings of the IEEE conference on computer vision and pattern recognition*, 2921–2929.

6 Supplementary file

In this file, we first provide experimental details on both COCO and Cityscapes. Then we give some visualization examples on two datasets.

6.1 Experimental details

COCO To make a fair comparison in Table 6, we add several additional components based on SpatialFlow in Table 5. Similar to UPSNet, we adopt deformable convolutions and the multi-scale trick. For deformable convolution, we apply it in the last three stage of ResNet-101, while the implementation in sub-networks is little different. In sub-networks, we want to fully leverage the spatial context and task-specific context, thus we first combine the spatial information flow and the task-specific feature, then use the combined feature to generate the offsets for the deformable convolution on the task-specific sub-network. The processes in sub-networks can be formulated as follow:

$$\begin{aligned}
 P_{regi,j} &= \zeta(P_{regi,j-1}); \\
 P_{cls_i,j} &= \zeta_{dcn}(P_{cls_i,j-1}, \phi_{offset}(P_{regi,j} + P_{cls_i,j-1})); \\
 P_{stuff_i,j} &= \zeta_{dcn}(P_{stuff_i,j-1}, \phi_{offset}(P_{regi,j} + P_{stuff_i,j-1})); \\
 P_{mask_{i,1}} &= \zeta(P_i + \psi(P_{stuff_{i,4}}), \phi_{offset}(P_{regi,4} + P_i)); \\
 P_{regi,0} &= P_i, \quad P_{cls_{i,0}} = P_i, \quad P_{stuff_{i,0}} = P_i.
 \end{aligned} \tag{6}$$

Here, ζ_{dcn} represents deformable convolution, ϕ_{offset} means an adaptation convolution, which generates offsets for deformable convolution. For multi-scale trick, we feed multi-scale images for SpatialFlow, and the scales are (1500, 1000), (1800, 1200), and (2100, 1400) with horizontal flip. For the hyper-parameters of SpatialFlow in the inference stage, we set the confidence score threshold for instance mask as 0.37, set the overlap threshold of instance masks as 0.37, and set the area limit threshold of stuff regions as 4900.

Cityscapes In Table 7, we adopt COCO pre-trained model on Cityscapes. To obtain the result of 62.5 PQ on Cityscapes *val* split, we first replace the convolution layers in stuff with deformable convolutions as UPSNet does, then we follow the steps below: (1) Finetune the COCO pre-trained model. As the number of things and stuff classes in Cityscapes is smaller than the number in COCO, 11/8 vs. 80/53, we have to finetune the layers that related to the number of classes. We freeze the rest layers and use a learning rate of 2.5×10^{-3} to train for 2 epochs. (2) Train the finetuned model as the standard SpatialFlow does. (3) Apply the multi-scale trick. The scales that we use in Cityscapes are (2304, 1152), (2432, 1216), (2560, 1280), and (2688, 1344) with horizontal flip. For the hyper-parameters on Cityscapes, we

set the confidence score threshold for instance mask as 0.37, set the overlap threshold of instance masks as 0.25, and set the area limit threshold of stuff regions as 2048.

6.2 Results visualization

We show some visualization examples of SpatialFlow on COCO and Cityscapes in Figure 5 and Figure 6 respectively.

Figure 5: We present the panoptic results on COCO *val* split.

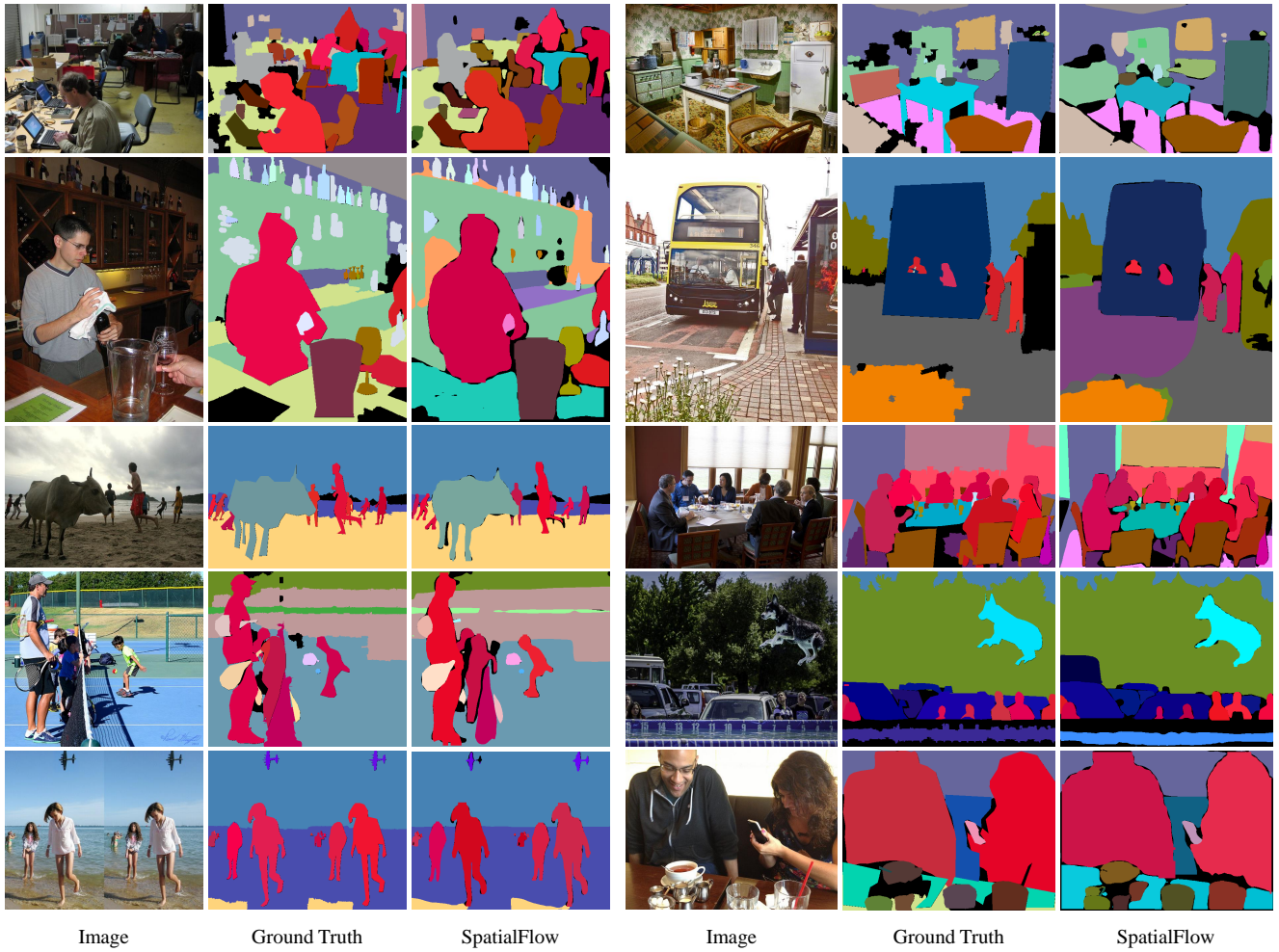
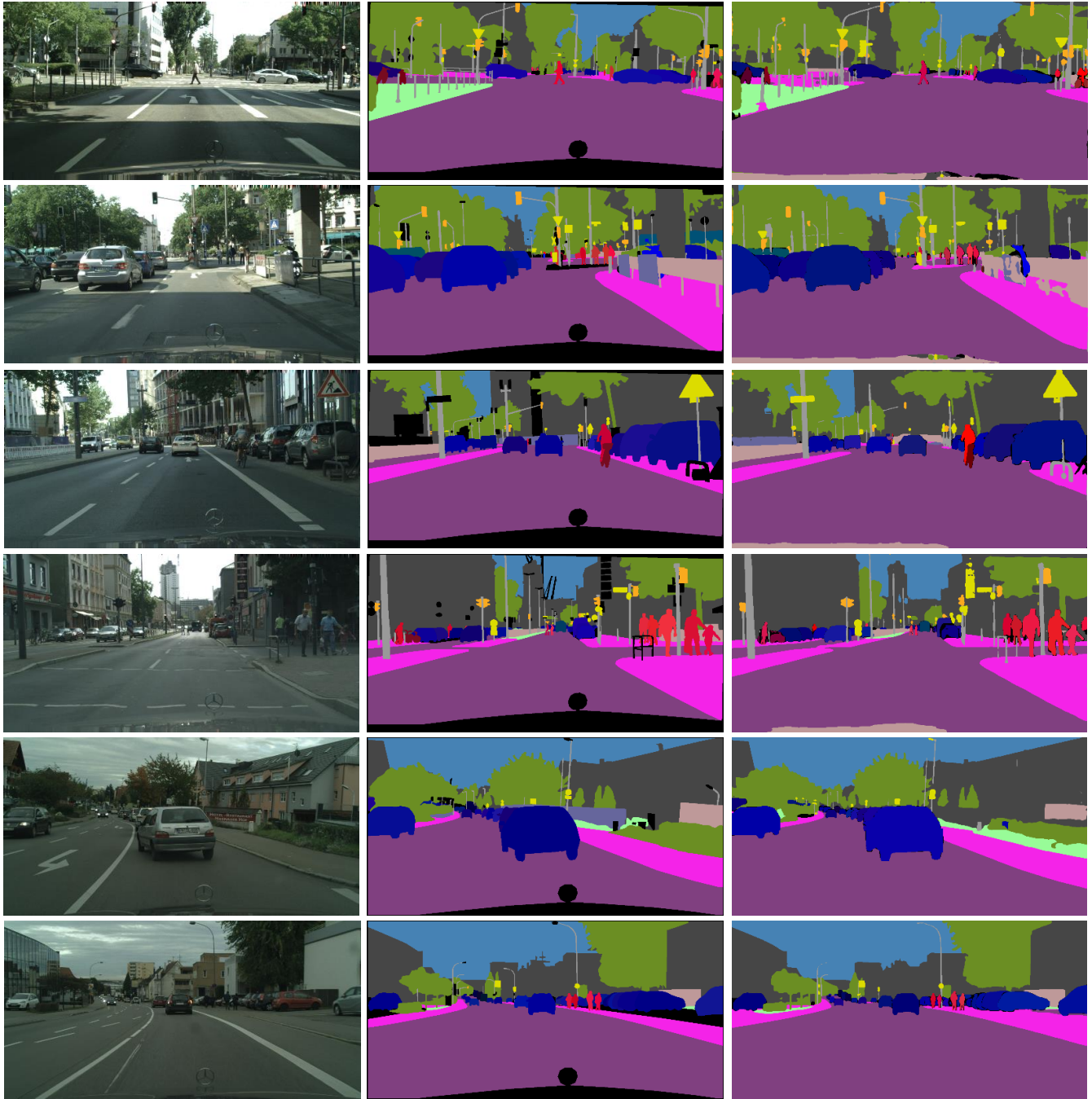


Figure 6: We present the panoptic results on Cityscapes *val* split.



Image

Ground Truth

SpatialFlow